SiO_2/Si(001) studied by time-resolved valence band photoemission at MHz repetition rates: Linear and nonlinear excitation of surface photovoltage

Robin Kamrla, Andreas Trützschler, Michael Huth, Cheng-Tien Chiang, Frank O. Schumann, and Wolf Widdra

Citation: Journal of Vacuum Science & Technology A **37**, 021101 (2019); doi: 10.1116/1.5082188
View online: https://doi.org/10.1116/1.5082188
View Table of Contents: https://avs.scitation.org/toc/jva/37/2
Published by the American Vacuum Society

SiO_2/Si(001) studied by time-resolved valence band photoemission at MHz repetition rates: Linear and nonlinear excitation of surface photovoltage

Robin Kamrla,[1,2] Andreas Trützschler,[1,2] Michael Huth,[2] Cheng-Tien Chiang,[1,2,a)]
Frank O. Schumann,[2] and Wolf Widdra[1,2,b)]
[1]*Institute of Physics, Martin-Luther-Universität Halle-Wittenberg, Von-Danckelmann-Platz 3, D-06120 Halle (Saale), Germany*
[2]*Max Planck Institute of Microstructure Physics, Weinberg 2, D-06120 Halle (Saale), Germany*

(Received 19 November 2018; accepted 14 January 2019; published 1 February 2019)

The authors investigate the fluence and doping dependence of the surface photovoltage (SPV) shifts at SiO_2/Si(001) interfaces by time-resolved photoelectron spectroscopy. Charge carriers are excited by pumping photon energies of $h\nu_{pump} = 1.2$ and 2.4 eV and probed by high-order harmonics of $h\nu_{probe} = 22.6$ eV at 0.2 and 0.7 MHz repetition rates. The authors observe SPV shifts of the nonbonding O_{2p} state by 240 meV for SiO_2/p-Si and by −140 meV for SiO_2/n-Si upon pumping with $h\nu_{pump} = 1.2$ eV, and their decay rate is estimated from time-resolved measurements. Moreover, the authors observe a striking pumping fluence dependence of SPV at these interfaces, which indicates charge carrier generation by both linear and nonlinear optical excitations. *Published by the AVS.*
https://doi.org/10.1116/1.5082188

I. INTRODUCTION

Interface states and oxygen vacancies within the SiO_2 layer terminating a Si(001) substrate have been of great interest over the last decades due to their ability to trap charge carriers with a prolonged lifetime and the resultant speed limitations of microelectronics.[1–5] With fs light excitations, electron dynamics at these interfaces can be triggered by linear optical absorption, whereas at high excitation intensity, multiphoton processes can play an important role.[6,7]

With high-order harmonic generation (HHG) as an alternative light source to synchrotron radiation for time-resolved photoelectron spectroscopy (tr-PES), it is possible to resolve the dynamics of charge carrier excitation and recombination in the valence band of semiconductors and metals.[8–14] Since HHG-based tr-PES is sensitive to surfaces and interfaces, it is an ideal tool for studying charge dynamics at ultrathin semiconductor–insulator heterostructures under linear and nonlinear excitation conditions.[15] At the interface of these heterostructures, electron dynamics is associated with the time-dependent charge trapping and band bending upon optical pumping. As a result, the surface photovoltage (SPV) effect occurs and the energy levels of all electronic states undergo an electrostatic shift on a time scale ranging from several ps to few μs.[5,8,10,16–27]

Here, we report HHG-based tr-PES measurements of the SPV on SiO_2/Si(001) driven by linear and nonlinear photoexcitation. We observe shifts of oxygen valence bands in SiO_2 pinned by the SPV at the interface. Moreover, we study its dependence on the doping of Si as well as the excitation density and photon energy. Our experiments reveal the important role of nonlinear optical excitations at semiconductor–insulator interfaces, which may provide insights for applications of nonlinear optoelectronic devices.

a)Electronic mail: cheng-tien.chiang@physik.uni-halle.de
b)Electronic mail: wolf.widdra@physik.uni-halle.de

II. EXPERIMENT

The experiments were driven by an ytterbium-fiber laser system (Impulse, Clark-MXR, Inc., USA), providing pulses of 1.2 eV photon energy at repetition rates between 0.2 and 1.0 MHz and an intensity full width at half maximum (FWHM) of 300 fs. By passing through a beamsplitter, the total output power was divided into pump and probe beam paths, which were overlapped on the sample in an ultrahigh vacuum chamber with a base pressure better than 5×10^{-10} mbar.

In the probe beam path, the laser output was used to drive HHG of vacuum-ultraviolet light between 14 and 42 eV.[28,29] To measure the valence band photoelectron spectra of SiO_2/Si(001), the 19th harmonic at a photon energy of $h\nu_{probe} = 22.6$ eV was selected via a toroidal diffraction grating and focused onto the sample. Due to the pulse front tilting at this diffraction geometry, we estimate the time resolution of the HHG beam to be about 2 ps.[12] To trigger SPV at the SiO_2/Si(001) interface, we used pumping photon energies of $h\nu_{pump} = 1.2$ or 2.4 eV. By varying the length of the pump beam path, time-resolved pump–probe measurements were performed at room temperature ($T = 300$ K). The angle of incidence for pump and probe beams at the sample surface was −45° and +45°, respectively. Due to the 90° angle between pump and probe beams at the surface, the finite spatial beam size will impose a limit of temporal resolution due to the noncollinear geometry between the wave fronts. This aspect will be estimated later in Sec. III B. The photoelectrons were detected by a commercial time-of-flight spectrometer with ±15° acceptance angle (Themis 1000, SPECS, Germany), which is aligned to the surface normal. The energy resolution of the experiments can be estimated by the band width of the high-order harmonics of around 70 meV.[30]

The p- and n-doped Si(001) samples with $n_p = 2 \times 10^{15}$ cm^{-3} boron and $n_n = 5 \times 10^{15}$ cm^{-3} phosphorus dopants were cleaned by Ar ion sputtering and heated up to 1100 K under UHV condition. The structure of the surfaces was

checked by low energy electron diffraction, indicating a (2×1) surface reconstruction.[31] Furthermore, the stoichiometry of the surfaces was verified by Auger spectroscopy and x-ray photoelectron spectroscopy. Subsequently, the SiO_2/p-Si and SiO_2/n-Si interfaces were prepared by exposure to 100 L of oxygen at 900 K. According to previous studies by Pi *et al.*, this procedure results in 15 Å thick SiO_2 layers on top of the Si.[32]

The pump fluence absorbed by the sample was estimated from the measured pump power P and the two dimensional intensity profile of the pump beam. Since the spatial extent of the probe beam with $d_{\mathrm{FWHM}} = 60\,\mu$m is much smaller than the pump beam diameters of $d_{\mathrm{FWHM}} > 0.5$ mm, the absorbed pump fluence within the probed sample area is given by

$$\Phi = \frac{P}{f_{Rep} \cdot 2\pi\sigma_{\perp}\sigma_{\parallel}} \cdot (1 - R), \tag{1}$$

where f_{Rep} is the repetition rate, R is the reflectance, and $\sigma = d_{\mathrm{FWHM}}/\sqrt{8\ln 2}$ is the standard deviation parallel ($\sigma_{\parallel}$) and perpendicular ($\sigma_{\perp}$) to the plane of incidence. For $h\nu_{pump} =$ 1.2 and 2.4 eV, we take the reflectance for p-polarized light at the 45° angle of incidence as $R = 0.2$ and $R = 0.3$, respectively.[33]

III. RESULTS

A. Doping dependence of SPV

Figure 1 shows the valence band photoelectron spectra in the energy range of the nonbonding O_{2p} state of SiO_2 for p- and n-doped Si(001) measured with $h\nu_{probe} = 22.6$ eV at a repetition rate of $f_{Rep} = 0.7$ MHz.[34] Both samples are illuminated with $h\nu_{pump} = 1.2$ eV at a fluence of 71 μJ/cm^2 and probed at a delay of $\Delta t = +350$ ps. Upon pumping, there is a clear shift of the spectra with its direction depending on the doping. For evaluation of the SPV shift, the spectra were fitted as indicated by the dotted curves. These fits correspond to the valence band edge positions of the O_{2p} nonbonding states, and their shape is provided by numerical interpolation of the spectra without pumping as shown by the dotted curves for the gray data points in Figs. 1(a) and 1(b). The spectra measured with pumping (black) are fitted by these fit-curves with an additional energy shift as the fitting parameter. The analysis in Fig. 1 reveals an SPV shift of $E_{SPV} = 240$ meV at SiO_2/p-Si and −140 meV at SiO_2/n-Si. At this specific pumping fluence, the results are in quantitative agreement with previous studies at Si 2p core levels.[25,35,36]

B. Dependence of SPV on pump–probe delay

The observed E_{SPV} strongly depends on the time delay between the pump and probe excitations. For $h\nu_{pump} = 1.2$ eV at $f_{Rep} = 0.2$ MHz and $h\nu_{pump} = 2.4$ eV at $f_{Rep} = 0.7$ MHz, the measured E_{SPV} on SiO_2/p-Si(001) is shown as a function of pump–probe delay in Figs. 2(a) and 2(b), respectively. Both datasets exhibit a monotonic increase of E_{SPV} at negative time delays $\Delta t < 0$ followed by a plateau for $\Delta t > 0$. Due to the ±45° angle of incidence and the pulse width of pump and probe beams, we can estimate a total time resolution of about 5 ps. Therefore, the slow increase at $\Delta t < 0$ is not a result of limited time resolution as will be discussed below.

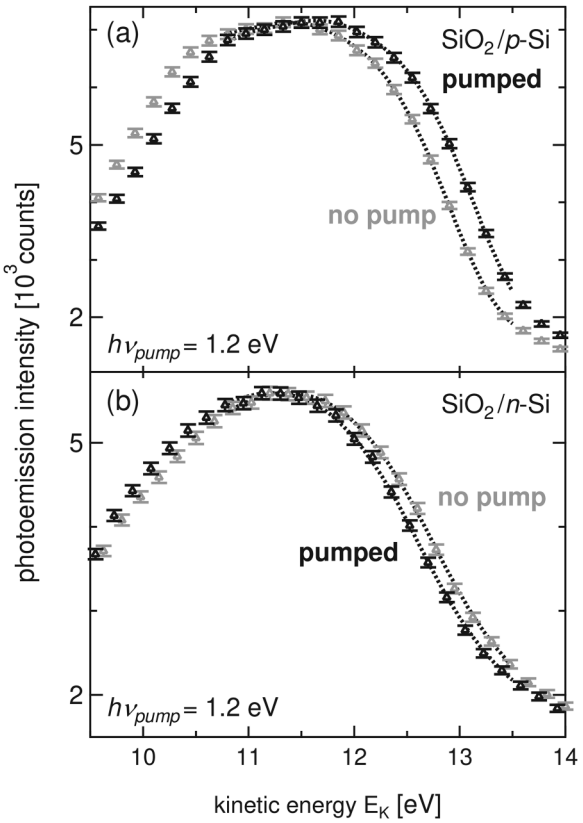

FIG. 1. Valence band photoelectron spectra of (a) SiO_2/p-Si(001) and (b) SiO_2/n-Si(001) with (black) and without (gray) pumping by $h\nu_{pump} =$ 1.2 eV at an absorbed fluence of 71 μJ/cm^2. The probe beam of $h\nu_{probe} =$ 22.6 eV was delayed from the pump by $\Delta t = +350$ ps. Dotted curves show the fits for the quantitative evaluation of E_{SPV}.

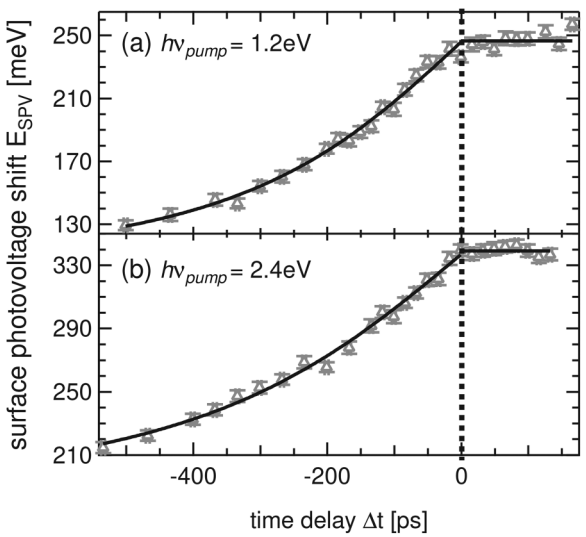

FIG. 2. Time dependence of the SPV at SiO_2/p-Si(001) for excitation with (a) $h\nu_{pump} = 1.2$ eV at a fluence of 53 μJ/cm^2 and (b) $h\nu_{pump} = 2.4$ eV at a fluence of 2 μJ/cm^2. Black curves at $\Delta t < 0$ are fits according to Eq. (3) with $E_{max} = 250$ meV, $E_{min} = 100$ meV, $r = 0.8$ mm in (a) and $E_{max} = 340$ meV, $E_{min} = 180$ meV, $r = 0.9$ mm in (b), respectively.

The rise at negative delays can be explained in terms of a pump-induced dipole field at the surface of the sample.[25] This dipole field is generated by the SPV shift upon pumping, and its spatial extent depends on the pump beam radius r. The temporal change of the surface potential causes a time-varying electrostatic field that interacts with the photoelectrons that were already emitted into vacuum. The electrostatic field will accelerate or decelerate the photoelectrons according to Ref. 25

$$\Delta E_K(\Delta t) = E_{max} + (E_{max} - E_{min}) \cdot \frac{\Delta t}{\sqrt{\frac{r^2}{v^2} + \Delta t^2}}, \tag{2}$$

where v is the velocity of the emitted photoelectrons. E_{min} and E_{max} represent the SPV before ($\Delta t \to \infty$) and right at ($\Delta t = 0$) the pump pulse. According to Eq. (2), the data in Figs. 2(a) and 2(b) for $\Delta t < 0$ can be fitted as indicated by the black curves, using simplified circular pump beam diameters of $r = 0.8$ and 0.9 mm, respectively. These values are in reasonable agreement with the measured FWHM of the pump beam Gaussian profile of 0.6 and 0.7 mm. The nearly constant E_{SPV} in Figs. 2(a) and 2(b) at positive delays $\Delta t > 0$ is due to the low recombination rate of excited charge carriers on the μs time scale.[36]

C. Intensity dependence of SPV

For pump photon energies of $h\nu_{pump} = 1.2$ and 2.4 eV, the dependence of E_{SPV} on the pumping fluence is shown in Figs. 3(a) and 3(b), respectively. In both cases, various

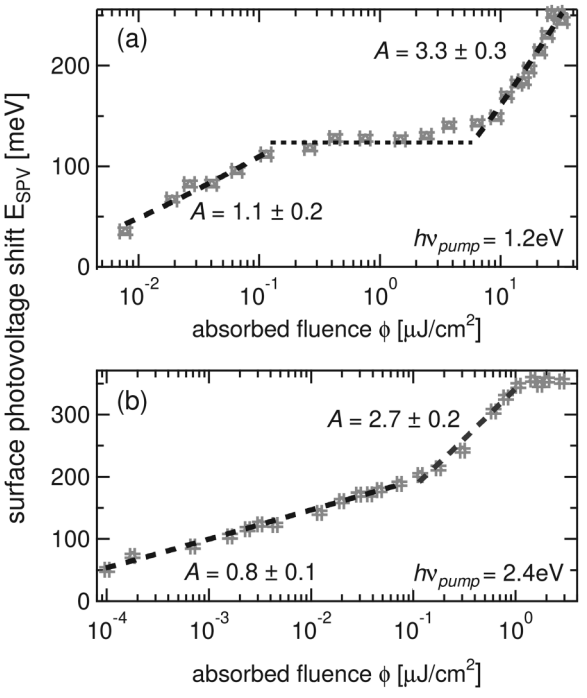

FIG. 3. Fluence dependence of E_{SPV} at SiO_2/p-Si(001) for excitation with (a) $h\nu_{pump} = 1.2$ eV at $f_{Rep} = 0.2$ MHz and (b) $h\nu_{pump} = 2.4$ eV at $f_{Rep} = 0.7$ MHz. The probe beam is delayed by $\Delta t = +150$ ps with respect to the pump. Black dashed curves are fits with Eq. (4). The horizontal dotted line in (a) marks the plateau at intermediate fluence.

regimes with linear dependences of E_{SPV} on $\log(\Phi)$ having different slopes can be identified, as explained in the following in accordance with earlier studies.[36,37] Upon pumping, an additional charge carrier density Δp is induced in Si, resulting in a relative change of charge carrier density $\Delta_p = \Delta p/n_p$ that is related to E_{SPV} at a limiting case of $kT \ll E_{SPV} \ll V_0$ by[37]

$$\Delta_p = \frac{E_{SPV}}{kT} \cdot e^{E_{SPV}/kT} \cdot e^{-V_0/kT}, \tag{3}$$

where V_0 is the equilibrium band bending and kT is the thermal energy at the sample temperature T. Due to the complicated dependence of Δ_p on E_{SPV}, $E_{SPV}(\Delta_p)$ cannot be expressed analytically. Since $kT \ll E_{SPV} \ll V_0$, the linear term in Eq. (3) in front of the exponential functions can be neglected and E_{SPV} depends logarithmically on Δ_p. By assuming the amount of excited charge carriers and a Δ_p that has a power-law dependence on the absorbed pumping fluence Φ,[38] $E_{SPV}(\Phi)$ can be approximated by[36]

$$E_{SPV}(\Phi) = AkT \cdot \ln(1 + B\Phi), \tag{4}$$

where A and B are fitting parameters. At low (high) excitation density, this formula ensures the linear (logarithmic) dependence of E_{SPV} on Δ_p in Eq. (3).

The dashed lines in Fig. 3 are fits of $E_{SPV}(\Phi)$ according to Eq. (4). For $\Phi < 0.2\,\mu J/cm^2$ at $h\nu_{pump} = 1.2$ eV, the data in Fig. 3(a) can be well described with $A = 1.1 \pm 0.2$ and $B = 0.4 \pm 0.2\,cm^2/nJ$, and for $\Phi > 10\,\mu J/cm^2$ with $A = 3.3 \pm 0.3$ and $B = 0.6 \pm 0.1\,cm^2/\mu J$. In the intermediate fluence range, E_{SPV} stays nearly constant. In strong contrast, E_{SPV} triggered by $h\nu_{pump} = 2.4$ eV in Fig. 3(b) only shows two regimes separated by $\Phi = 0.1\,\mu J/cm^2$ with $A = 0.8 \pm 0.1$ ($B = 120 \pm 30\,cm^2/nJ$) and $A = 2.7 \pm 0.2$ ($B = 120 \pm 40\,cm^2/\mu J$), which will be discussed in detail later. For Φ above $2\,\mu J/cm^2$, the E_{SPV} saturates at 350 meV and corresponds to a complete lifting of the band bending at the SiO_2/p-Si(001) interface known as flat-band condition.[25,35,36]

IV. DISCUSSION

A. Doping dependence of SPV

The E_{SPV} on the p- and n-doped samples in Fig. 1 differs clearly in sign as well as in magnitude. This behavior can be explained according to previous experimental and theoretical studies on P_{b0} and P_{b1} states at the SiO_2/Si interfaces.[1–5] These defect states result from Si dangling-bonds at the interface and are distributed in the lower and upper half of the Si bandgap, respectively.[5]

Following the analysis of Long *et al.* for time-resolved core level photoemission,[37] these interface states in the band gap of Si lead to a pinning of the Fermi level at the SiO_2/ Si interface. As a result, a space charge region is formed in Si near the interface, and bands are bent from the interior of Si toward the interface.[39] At 300 K, the Fermi level of bulk p- and n-Si is located approximately 230 meV above the valence band and 230 meV below the conduction band, respectively. Therefore, the Si bands at the SiO_2/p-Si interface are bent toward lower energies and at SiO_2/n-Si toward

higher energies. Upon illumination, photoexcited electron–hole pairs are generated and then separated within the space charge region.[39] Due to the band bending, the photoexcited minority charge carriers are accumulated at the interface whereas the majority charge carriers are accelerated into the bulk. This charge separation counteracts on the band bending and leads to a screening of the space charge potential by the photoexcited charge carriers. Finally, the band bending becomes lifted and the resultant electrostatic shift of the electronic states at the interface propagates into the SiO_2 overlayer. Because of this electrostatic shift of the electronic states in SiO_2, the kinetic energies E_K of photoelectrons from the nonbonding O_{2p} state are shifted to higher energies for SiO_2/p-Si and to lower energies for SiO_2/n-Si as displayed in Figs. 1(a) and 1(b), respectively. In addition, the differences in the magnitude of E_{SPV} for SiO_2/p-Si and SiO_2/n-Si can be related to an asymmetrically distributed interface state density, which has been pointed out by the work of Edwards.[1]

B. Decay of SPV

Here, we discuss the quantitative evaluation of carrier decay time that can be extracted from the time-resolved SPV measurements in Fig. 2. Following the approach of Hecht,[40] the decay of E_{SPV} is governed by thermionic emission whose probability scales exponentially with E_{SPV} itself. This leads to a lifetime τ depending on E_{SPV} as $\tau(E_{SPV}) = \tau_\infty e^{-E_{SPV}/\alpha' kT}$.[36,41] In this formula, τ_∞ describes the material dependent dark carrier lifetime and α' is a phenomenological correction factor between 1 and 2, similar to the ideality factor of Schottky diodes.[25,36,42,43] By using τ, a decay equation for Δ_p can be formulated as

$$\frac{d\Delta_p(t)}{dt} = -\frac{\Delta_p(t)}{\tau(E_{SPV})} = -\frac{\Delta_p(t)}{\tau_\infty}\cdot e^{E_{SPV}/\alpha' kT}. \tag{5}$$

In order to describe the time-resolved measurements in Sec. III B, the relation between Δ_p and E_{SPV} in Eq. (3) is modified as

$$\Delta_p(E_{SPV}) = \frac{E_{SPV}}{\alpha kT}\cdot e^{E_{SPV}/\alpha kT}\cdot e^{-V_0/kT} \tag{6}$$

by adding a parameter α, which plays a similar role as the fitting parameter A in Eq. (4). It has been shown in previous studies that one can describe the decay of E_{SPV} analytically by neglecting the linear term in Eq. (6) and formulate $E_{SPV}(\Delta_p)$ similarly as in Eq. (4).[36] Here, we derive a solution of Eq. (5) with α and α' as independent parameters, since they may differ from each other and α can be estimated from experiment similar to A in Eq. (4).

Assuming $\Delta_p(E_{SPV})$ to be a continuous and monotonic function, one can derive a differential equation for the decay of E_{SPV} as

$$\frac{dE_{SPV}(t)}{dt} = \left(\frac{d\Delta_p(E_{SPV})}{dE_{SPV}}\right)^{-1}\cdot\frac{d\Delta_p(t)}{dt}. \tag{7}$$

Inserting the derivative of Eq. (6) with respect to E_{SPV} as well as the relation in Eq. (5) into Eq. (7), we arrive at an analytical differential equation for the time dependence of E_{SPV}

$$\frac{dE_{SPV}(t)}{dt} = -\frac{1}{\tau_\infty}\cdot\frac{E_{SPV}}{1+E_{SPV}/\alpha kT}\cdot e^{E_{SPV}/\alpha' kT}. \tag{8}$$

At a limiting case of $E_{SPV} \gg \alpha kT$, this differential equation can be solved as

$$E_{SPV}(t) = -\alpha' kT\cdot\ln\left(\frac{\alpha t}{\alpha'\tau_\infty} + e^{-E_{SPV,0}/\alpha' kT}\right), \tag{9}$$

with a given initial condition $E_{SPV}(t=0) = E_{SPV,0}$.

From the measurements presented in Fig. 2, we find $E_{SPV,0} = E_{max}$ at $t = 0$ and derive the value of SPV shift shortly before the subsequent laser pulse reaches the sample at $t = f_{Rep}^{-1}$ as $E_{SPV}(f_{Rep}^{-1}) \approx E_{min}$. Inserting these conditions into Eq. (9), τ_∞ can be expressed as

$$\tau_\infty = \alpha\cdot\left[\alpha' f_{Rep}\cdot\left(e^{-E_{min}/\alpha' kT} - e^{-E_{max}/\alpha' kT}\right)\right]^{-1}. \tag{10}$$

In order to estimate τ_∞ quantitatively from our experimental results, we assume $\alpha = A$ for the measurements pumped by $h\nu_{pump} = 1.2$ and 2.4 eV with $A = 1.1$ and $A = 0.8$, respectively, which are extracted from Fig. 3 in the low fluence regime. The role of A at higher excitation densities will be discussed in Sec. IV C. In addition, we assume $\alpha' = 2$ according to previous works,[25,36] and we obtain $\tau_\infty = 18$ and 19 μs for $h\nu_{pump} = 1.2$ and 2.4 eV, respectively. These values are in agreement with time-resolved data measured by Shavorskiy *et al.*[44] on a 10 Å native oxide layer of $\tau_\infty = 20\,\mu$s at $E_{SPV,0} = 250$ meV. Using Eq. (9), we are also able to describe the time-dependent decay of E_{SPV} as measured on SiO_2/p-Si by Bröcker *et al.*,[36] which is shown in Fig. 4. The fit to the experimental data leads to $\tau_\infty \approx 19\,\mu$s in agreement with the data discussed above.

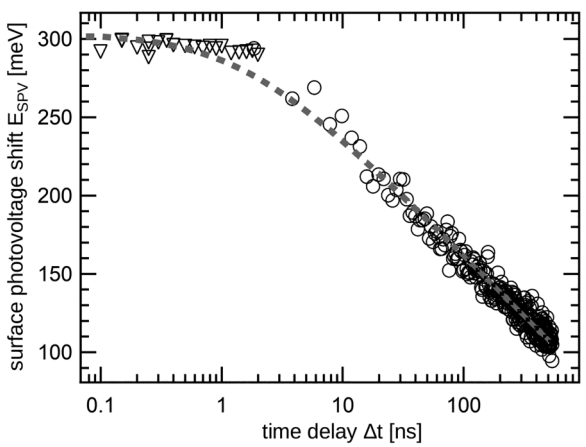

FIG. 4. Time dependence of the surface photovoltage E_{SPV} on pump–probe delay Δt. The gray dashed curve shows a fit according to Eq. (9) with $E_{SPV,0} = 300$ meV, $\alpha = 2$, $\alpha' = 1.3$, and $\tau_\infty = 19\,\mu$s. Symbols are data for SiO_2/p-Si(001) from Bröcker *et al.* (Ref. 36) with $h\nu_{pump} = 2.3$ eV (data reproduced with permission from Ref. 36).

C. Linear and nonlinear excitation of charge carriers

In order to explain the slopes of the fluence-dependent results in Fig. 3, we consider nonlinear absorption of m photons for photoexcitation of a single electron–hole pair, i.e., $\Delta_p \propto \Phi^m$. Taking this nonlinear scaling explicitly into account, Eq. (3) can be approximated analogously to Eq. (4) as

$$E_{SPV}(\Phi) = m \cdot AkT \cdot \ln(1 + B\Phi). \tag{11}$$

Here, we assign the low fluence regimes of $h\nu_{pump} = 1.2$ and 2.4 eV in Fig. 3 to linear excitation with one single photon ($m = 1$) and the high fluence regime to nonlinear three-photon excitation with $m = 3$. In addition, we assume a constant A for different regimes. To describe the overall pump fluence dependence of SPV in Fig. 3, we estimate the pump-induced relative change of carrier density Δ_p by the absorption length l_{abs} at $h\nu_{pump}$ as[36]

$$\Delta_p = \frac{\gamma_1 \Phi + \gamma_3 \Phi^3}{n_p \cdot l_{abs} \cdot h\nu_{pump}}, \tag{12}$$

where n_p is the density of dopants and γ_1 and γ_3 are scaling factors corresponding to the cross section of linear and three-photon excitations.

In Fig. 5(a), the data from Fig. 3 are plotted versus $\Delta_{p,lin}$ according to Eq. (12) with $\gamma_3 = 0$ and $\gamma_1 = 1$ for linear excitation. In comparison, the same data are shown in Fig. 5(b) according to Eq. (12) taking nonlinear excitation of charge carriers into account. For $h\nu_{pump} = 1.2$ eV at low fluence, we assume $\Delta_{p,multi} = \Delta_{p,lin}$, because linear excitation dominates over the nonlinear one. Since E_{SPV} in Fig. 3(a) stays constant at intermediate fluence, we assume no further changes in $\Delta_{p,multi}$ from linear charge carrier excitation whose origin will be explained later. At higher fluences for $E_{SPV,0} \geq 125$ meV, $\Delta_{p,multi}$ is calculated from Eq. (12) by $\gamma_1 = 0$ and $\gamma_3 = 6.6 \cdot 10^{-4}\,\mathrm{cm}^4/\mu\mathrm{J}^2$. In Fig. 5(b) for $h\nu_{pump} = 2.4$ eV, we use $\gamma_1 = 1$ and $\gamma_3 = 93\,\mathrm{cm}^4/\mu\mathrm{J}^2$.

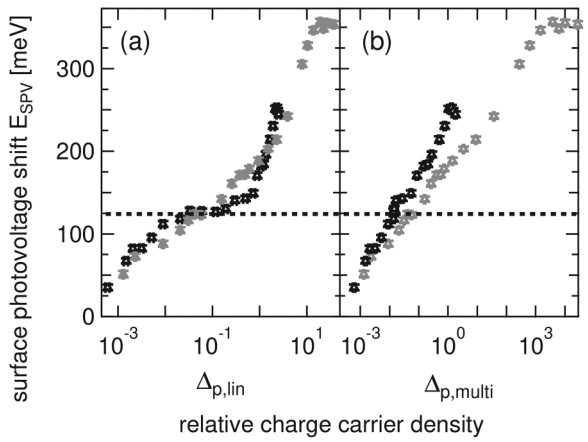

FIG. 5. Dependence of E_{SPV} at SiO_2/p-Si(001) on the relative charge carrier density excited by linear and nonlinear optical absorption $\Delta_{p,lin}$ (a) and $\Delta_{p,multi}$ (b), respectively. Data points in black from Fig. 3(a) and in gray from Fig. 3(b) are scaled according to Eq. (12). The dashed horizontal line marks the plateau of $E_{SPV} = 125$ meV for $h\nu_{pump} = 1.2$ eV at intermediate excitation density.

As one can clearly see in Fig. 5(b), the SPV for both $h\nu_{pump}$ is comparable when plotted as a function of $\Delta_{p,multi}$, indicating a well-defined general relation between the nonlinearly photoexcited carrier density and the SPV as formulated by Eq. (11).

For further analysis of the data shown in Fig. 5(a), the temporal relaxation of E_{SPV} discussed in Sec. IV B needs to be taken into account. Since the measurements with $h\nu_{pump} = 1.2$ eV are performed at $f_{Rep}^{-1} = 5\,\mu$s, at least five consecutive pumping pulses contribute to the measured SPV within the $\tau_\infty \approx 20\,\mu$s that was derived before. Therefore, at $\Delta_p \approx 0.2$, the density of total excited charge carriers equals to the concentration of boron dopants within the Si bulk. As can be seen in Fig. 5(a), this estimated value lies within the plateau of E_{SPV}, and therefore we ascribe the nearly constant E_{SPV} for $h\nu_{pump} = 1.2$ eV at the intermediate fluence to the complete excitation of all boron acceptor states. These states are located 45 meV above the Si valence band within the indirect bandgap $E_{gap} = 1.15$ eV of Si. At room temperature, these states are occupied by electrons before the photoexcitation with $h\nu_{pump} = 1.2$ eV.[1]

In the following, we will discuss the possible origin of the plateau. The boron acceptor states are localized in real space and consequently have a flat dispersion in the momentum space.[45,46] Therefore, optical excitation of electrons from the acceptor states into the conduction bands may not require phonons and could more efficiently generate charge carriers than the indirect transitions from the valence band to the conduction band of Si. However, due to the limited amount of dopants in Si, this contribution saturates at higher fluences when all electrons in the acceptor states are excited. Consequently, E_{SPV} does not further increase exponentially when Δ_p is approaching 0.2. At much higher fluences for $h\nu_{pump} = 1.2$ eV, the transition to $m = 3$ is observed in Fig. 3. There, the three-photon energy of 3.6 eV is sufficient to trigger direct transitions from the valence to the conduction bands of Si across the direct bandgap of 3.4 eV.

V. SUMMARY AND CONCLUSIONS

By using time-resolved photoelectron spectroscopy with a high-order harmonic light source working at megahertz repetition rates, we characterized the time, intensity, and doping dependence of surface photovoltage at the SiO_2/Si(001) interface upon sub-bandgap and above bandgap photoexcitation. At the SiO_2/p-Si interface, we observe an SPV shift of the nonbonding O_{2p} state of 240 meV toward higher energies upon illumination with $h\nu_{pump} = 1.2$ eV, whereas at SiO_2/n-Si, a shift of 140 meV toward lower energies is found. From the time-resolved measurements, we estimate the decay time of SPV at SiO_2/p-Si of about 20 μs for $h\nu_{pump} = 1.2$ and 2.4 eV. Moreover, we observe the transition from linear to nonlinear excitations of SPV, which leads to distinctly different scaling of SPV on the pumping fluence. Whereas in the regime of low excitation density, linear photoexcitation of charge carriers dominates; at high fluences, nonlinear optical excitations can occur. Our observation emphasizes the importance of nonlinear photoexcitations at

SiO_2/Si interfaces and may provide a deeper understanding of semiconductor–insulator heterostructures aiming at possible applications to nonlinear optoelectronic devices.

ACKNOWLEDGMENTS

The authors would like to gratefully acknowledge the valuable technical support from H. Menge, F. Helbig, F. Thiele, F. Weiß, and R. Kulla. This work is partially supported by the Deutsche Forschungsgemeinschaft through SFB 762 (B7, A3) and SFB/TRR 227 (A06).

[1]A. H. Edwards, Phys. Rev. B **36**, 9638 (1987).
[2]J. P. Campbell and P. M. Lenahan, Appl. Phys. Lett. **80**, 1945 (2002).
[3]C. R. Helms and B. E. Deal, *The Physics and Chemistry of SiO_2 and the Si-SiO_2 Interface* (Plenum, New York, 1988).
[4]E. Mehes and C. H. Patterson, Phys. Rev. Mater. **1**, 044602 (2017).
[5]T. Tsuchiya and Y. Ono, Jpn. J. Appl. Phys. **54**, 04DC01 (2015).
[6]T. Wang, N. Venkatram, J. Gosciniak, Y. Cui, G. Qian, W. Ji, and D. T. H. Tan, Opt. Express **21**, 32192 (2013).
[7]J. G. Mihaychuk, N. Shamir, and H. M. van Driel, Phys. Rev. B **59**, 2164 (1999).
[8]P. Siffalovic, M. Drescher, and U. Heinzmann, Europhys. Lett. **60**, 924 (2002).
[9]K. Oguri, K. Kato, T. Nishikawa, H. Gotoh, K. Tateno, T. Sogawa, and H. Nakano, Jpn. J. Appl. Phys. **51**, 072401 (2012).
[10]K. Oguri, T. Tsunoi, K. Kato, H. Nakano, T. Nishikawa, K. Tateno, T. Sogawa, and H. Gotoh, Appl. Phys. Express **8**, 022401 (2015).
[11]A. Melzer, D. Kampa, J. Wang, and T. Fauster, Phys. Rev. B **80**, 205424 (2009).
[12]M. Bauer, J. Phys. D Appl. Phys. **38**, R253 (2005).
[13]S. Hellmann *et al.*, Nat. Commun. **3**, 1069 (2012).
[14]C. W. Nicholson, A. Lücke, W. G. Schmidt, M. Puppin, L. Rettig, R. Ernstorfer, and M. Wolf, Science **362**, 821 (2018).
[15]J. V. Barth, G. Costantini, and K. Kern, Nature **437**, 671 (2005).
[16]B. M. Marsh, M. E. Vaida, S. K. Cushing, B. R. Lamoureux, and S. R. Leone, J. Phys. Chem. C **121**, 21904 (2017).
[17]B. F. Spencer *et al.*, Faraday Discuss. **171**, 275 (2014).
[18]S. Grafström, J. Appl. Phys. **91**, 1717 (2002).
[19]M. Moreno, M. Alonso, J. L. Sacedon, M. Höricke, R. Hey, K. Horn, and K. H. Ploog, Phys. Rev. B **61**, 16060 (2000).
[20]M. H. Hecht, Phys. Rev. B **43**, 12102 (1991).
[21]T. Watanabe, M. Hori, T. Tsuchiya, A. Fujiwara, and Y. Ono, Jpn. J. Appl. Phys. **56**, 011303 (2017).
[22]M. Marsi *et al.*, J. Electron. Spectrosc. Relat. Phenom. **94**, 149 (1998).
[23]C. Bandis and B. B. Pate, Surf. Sci. **345**, L23 (1996).
[24]T. J. Šarapatka, Surf. Sci. **275**, 443 (1992).
[25]W. Widdra *et al.*, Surf. Sci. **543**, 87 (2003).
[26]R. Yukawa, S. Yamamoto, K. Akikubo, K. Takeuchi, K. Ozawa, H. Kumigashira, and I. Matsuda, Adv. Mater. Interfaces **3**, 1600527 (2016).
[27]S. Tanaka, J. Electron. Spectros. Relat. Phenomena **185**, 152 (2012).
[28]C.-T. Chiang, A. Blättermann, M. Huth, J. Kirschner, and W. Widdra, Appl. Phys. Lett. **101**, 071116 (2012).
[29]C.-T. Chiang, M. Huth, A. Trützschler, M. Kiel, F. Schumann, J. Kirschner, and W. Widdra, New J. Phys. **17**, 013035 (2015).
[30]C.-T. Chiang, *Encyclopedia of Interfacial Chemistry*, edited by K. Wandelt (Elsevier, Oxford, 2018), pp. 28–38.
[31]T. Tabata, T. Aruga, and Y. Murata, Surf. Sci. **179**, L63 (1987).
[32]T.-W. Pi, J.-F. Wen, C.-P. Ouyang, R.-T. Wu, and G. Wertheim, Surf. Sci. **478**, L333 (2001).
[33]M. A. Green, Sol. Energy Mater. Sol. Cells **92**, 1305 (2008).
[34]F. G. Bell and L. Ley, Phys. Rev. B **37**, 8383 (1988).
[35]M. Copuroglu, H. Sezen, R. L. Opila, and S. Suzer, ACS Appl. Mater. Interfaces **5**, 5875 (2013).
[36]D. Bröcker, T. Gießel, and W. Widdra, Chem. Phys. **299**, 247 (2004).
[37]J. P. Long, H. R. Sadeghi, J. C. Rife, and M. N. Kabler, Phys. Rev. Lett. **64**, 1158 (1990).
[38]The corresponding power-law will be discussed in detail in Sec. IV B.
[39]S. M. Sze and K. K. Ng, *Physics of Semiconductor Devices* (Wiley, New York, 2006).
[40]M. H. Hecht, Phys. Rev. B **41**, 7918 (1990).
[41]R. J. Hamers and D. G. Cahill, J. Vac. Sci. Technol. B **9**, 514 (1991).
[42]W. Shockley and W. T. Read, Phys. Rev. **87**, 835 (1952).
[43]M. A. Kroon andR. A. C. M. M. van Swaaij, J. Appl. Phys. **90**, 994 (2001).
[44]A. Shavorskiy *et al.*, Rev. Sci. Instrum. **85**, 093102 (2014).
[45]J. C. Inkson, J. Phys. C Solid State Phys. **14**, 1093 (1981).
[46]D. M. Eagles, J. Phys. Chem. Solids **16**, 76 (1960).